Available online at www.sciencedirect.com
ScienceDirect
Journal of Power Sources 161 (2006) 1302–1306
JOURNAL OF POWER SOURCES
www.elsevier.com/locate/jpowsour

Polyanthra[1,9,8-b,c,d,e][4,10,5-b,c,d,e]bis-[1,6,6a(6a-S) trithia] pentalene-active material for cathode of lithium secondary battery with unusually high specific capacity

Z.J. Liu, L.B. Kong, Y.H. Zhou, C.M. Zhan *

College of chemistry and Molecular sciences, Wuhan University, Wuhan 430072, PR China

Received 30 November 2005; received in revised form 5 June 2006; accepted 8 June 2006
Available online 28 July 2006

Abstract

Polyanthra[1,9,8-b,c,d,e][4,10,5-b,c,d,e]bis-[1,6,6a(6a-S)trithia]pentalene (PABTP) was prepared and investigated as cathode active material for lithium secondary batteries. The organic disulfide polymer was prepared by the direct sulfurization of anthracene and the oxidative coupling polymerization of the sulfide anthracene, characterized by FT-IR, Raman, elemental analysis, XPS and XRD. The polymer was used as cathode active material and the lithium secondary batteries were assembled and tested. The polymer had high specific capacity up to 1500 mAh g^{-1}, which remained the value of 800 mAh g^{-1} at the 77th cycle, and kept high charge–discharge efficiency of 85% in the whole test.

Keywords: Lithium secondary battery; Cathode active material; Organodisulfide polymer; High discharge specific capacity

1. Introduction

The development of high, rechargeable batteries is currently the area of intense research both in academia and industry. Lithium metal has very high specific capacity (3700 mAh g^{-1}) as anode of lithium secondary batteries. To achieve lithium secondary battery with high energy density, high performance cathode materials are commanded. But the cathode active materials with high specific capacity matching that of lithium anode are still in absence. Therefore, cathode material with high specific capacity is the "bottleneck" to develop high energy density lithium secondary batteries. Organodisulfide compounds afford energy storage by reversible two-electron redox reaction of the disulfide bond (S–S) and have attracted intense research interests since 1990s [1–5]. Small molecules organic disulfides are easy to migrate from cathode and result in short lifetime. A widely investigated organic disulfide compound, 2,5-dimercapta-1,3,4-thiadiazole (DMcT), also forms small molecular fragments during charge process. Therefore, organic materials with stable polymeric backbone during redox reaction may promise good electron conductivity and longer cycle life. In fact, conductive polymers were used as electrodes very early, but the specific capacity was below 200 mAh g^{-1} [6–8]. Polyanilines with S–S bonds as side chains was synthesized and investigated as cathode active material in lithium batteries and showed high energy density, but the specific capacity was lower than that of theoretic value [9].

In a communication, we reported a novel cathode material polyanthra[1,9,8-b,c,d,e][4,10,5-b,c,d,e]bis-[1,6,6a(6a-S)trithia]pentalene (PABTP) for Lithium secondary batteries, which had specific capacity of 300 to 250 mAh g^{-1} and theoretic capacity of 440 mAh g^{-1} [10]. The material has several advantages to benefit the practical application: facile preparation, environmental benign, insolubility, abundant raw material and low price. Moreover, the charge and discharge are feasible in high efficiency at ambient conditions. Therefore, we work on the material and have got high specific capacity up to 1500 mAh g^{-1} from a new electrolyte system. In this paper, we report the new discovery and the preparation, characterization and electrochemistry performance in detail.

* Corresponding author. Tel.: +86 27 87219024; fax: +86 27 68754067.
E-mail addresses: yhzhou@chem.whu.edu.cn (Y.H. Zhou), zhancm@chem.whu.edu.cn (C.M. Zhan).

0378-7753/$ – see front matter © 2006 Elsevier B.V. All rights reserved.
doi:10.1016/j.jpowsour.2006.06.048

2. Experimental

2.1. Materials

Anthracene was purchased from Merck Co., Reagent grade of $LiN(CF_3SO_2)_2$ (LiTFSI), 1,3-dioxy-pentane (DXL), ethylene glycoldimethyl ether (DME) and all other reagents were purchased from commercial and used as received without further purification.

2.2. Characterization and electrochemical measurements

Elemental analysis was performed on VarioEL III instrument. FT-IR spectra were recorded on a NICOLET AVATAR360 FT-IR spectrometer with KBr pellets. Raman spectra were obtained from Laser Confocal Raman microspectroscopy with excitation wave number of 514.5 nm argon ion laser. X-ray photoelectron spectroscopy (XPS) analysis data were obtained with the magnesium source radiation (1253.6 eV) operating at 10 KV and 10 mA. The charge–discharge tests of the lithium secondary batteries were performed on LAND BATTERY TEST SYSTEM with current density of 40 mA g^{-1} in the voltage range of 1.4–4.4 V. To assemble the lithium batteries two electrodes system was applied using lithium as anode and the composite cohering on stainless steel foil as cathode with the area of 1.75 cm^2. The composite contained positive active material of 1.50 mg with the active material, acetylene carbon and poly(tetrafluoroethylene) (PTFE) in weight ratio of 4:4:2. The electrolyte solution was DXL–DME (2:1) containing 1 mol L^{-1} $LiN(CF_3SO_2)_2$. The batteries were assembled in dry glove box filled with argon.

2.3. Material preparation

2.3.1. Synthesis of ABTP and PABTP

The synthesis of anthra[1,9,8-b,c,d,e][4,10,5-b,c,d,e]bis-[1,6,6a(6a-S)trithia]pentalene (ABTP) and PABTP is shown in Scheme 1 and the following description. ABTP was prepared by solvent-free sulfurization of anthracene. In a dry three-neck flask equipped with condenser and nitrogen inlet, the mixture of 6 g sulfur and 1 g anthracene was heated at 300 ° for 6 h, the black solid with metal luster was collected and extracted with CS_2 in Soxhlet's extractor for 36 h to remove free sulfur and anthracene and obtained as the product ABTH.

PABTP was obtained by oxidative coupling polymerization of ABTP in the presence of $FeCl_3$ in anhydrous $CHCl_3$ solution for 36 h. After reaction, $CHCl_3$ was removed by filtering; $FeCl_3$ was eliminated by washing with dilute hydrochloric acid and distilled water to pH 7. The polymer was extracted by methanol in Soxhlet's extractor to remove $FeCl_3$ and dried at 80 °C in oven to constant weight.

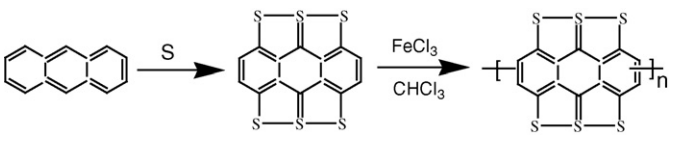

Scheme 1. Synthesis of polymer PABTP.

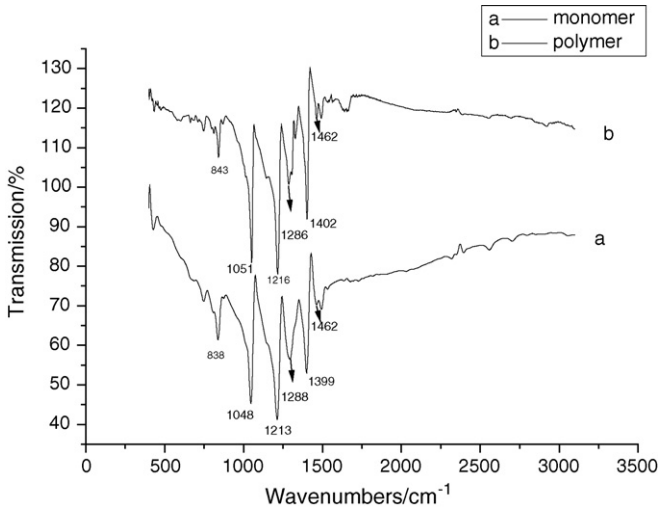

Fig. 1. IR spectra of: (a) monomer ABTP and (b) PABTP.

3. Results and discussion

3.1. Vibration spectra

The standard NMR technique is not available for the characterization of ABTP and PABTP because of their insolubility. The vibration spectroscopic characterization was performed and the IR spectra are shown in Fig. 1. FTIR spectra show strong C=S and C–S stretching vibration at 1213, 1048 cm^{-1} for ABTP and 1216, 1050 cm^{-1} for PABTP ,respectively. The C=C stretching vibration for the monomer and polymer can be found at 1399, 1462 and 1402, 1462 cm^{-1}, respectively. In addition, the peak at 838 cm^{-1} is attributed to the C–H out of space vibration for the adjacent hydrogen on the anthracene moieties, which became weak and shifted to 842 cm^{-1}, indicating the formation of isolated hydrogen due to the polymerization.

Fig. 2 shows the Raman spectra of ABTP and PABTP. The S–S stretching mode, observed at 463 and 462 cm^{-1} for the

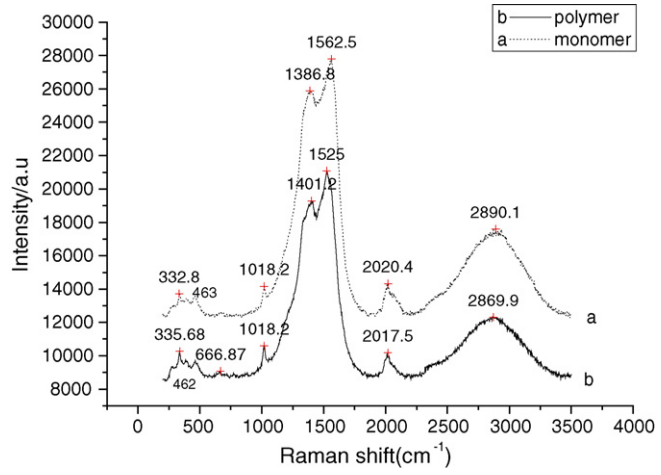

Fig. 2. Raman spectra of: (a) monomer ABTP and (b) PABTP.

monomer and polymer, respectively, providing evidence for the S–S bond in the compounds. Also the C–S stretching mode is observed at 667 and 661 cm^{-1}, respectively. The peak at 1018 cm^{-1} was assigned to the C=S vibration. In the C=C stretching region between 1200 and 1650 cm^{-1}, there are two main bands around 1400 and 1550 cm^{-1}.

Raman spectroscopy has been used to analyze the chain length dependence of the effective conjugation length in linear π-conjugated systems and established a linear dependence of the Raman shifts with the inverse conjugation length for oligomeric conjugated systems. Previous work on oligomeric conjugated systems of homogeneous structure, such as oligoenes, oligopyrroles, thiophene-based π-conjugated oligomers, the C=C stretching frequency was found to downshift by 10–130 cm^{-1} with increasing conjugated chain length [11–15]. Comparing the stretching vibrations of C=C for ABTP and PABTP, one can found that the main stretching vibration frequency shifted from 1562 to 1525 cm^{-1} after polymerization, downshift by 37 cm^{-1},indicating the increasing of conjugated chain length. The obvious downshift of main C=C vibration can be an evidence of polymerization of ABTP.

3.2. Elemental analysis, intrinsic viscosity and electrical conductivity

To improve the cycle life and the electric conductivity of the ABTP-containing materials, polymerization of the ABTP was conducted. Because of their insolubility in organic solvents, molecular weight measurement is difficult. However, the polymerization of ABTP is supported by the intrinsic viscosity and elemental analysis results. From a carefully treated ABTP and its polymer PABTP, the H-content was 0.817% (calcd.: 1.10%) and 0.606% (calcd.: 0.55%), respectively, indicating there was a de-hydrogenized polymerization. In addition, the intrinsic viscosity of 0.31 L g^{-1} was measured for PABTP in aqueous sodium sulfide at 26 °C, which strongly suggested its polymeric structure. Finally, the electrical conductivity of PABTP was higher than that of ABTP. Doping with iodine and measured at room temperature, the electrical conductivity of PABTP is 1.52×10^{-4} S cm^{-1} while ABTP is 7.38×10^{-6} S cm^{-1}, two order of magnitude higher than that of its monomer. These results indicate the larger π-conjugation system due to the polymerization. Because of fused sulfur-containing aromatic rings and the formation of charge-transfer complex with iodine, ABTP has fair electrical conductivity. After polymerization, more ABTP linked together to form conjugated polymeric backbone, which result the larger aromatic system and the higher electrical conductivity.

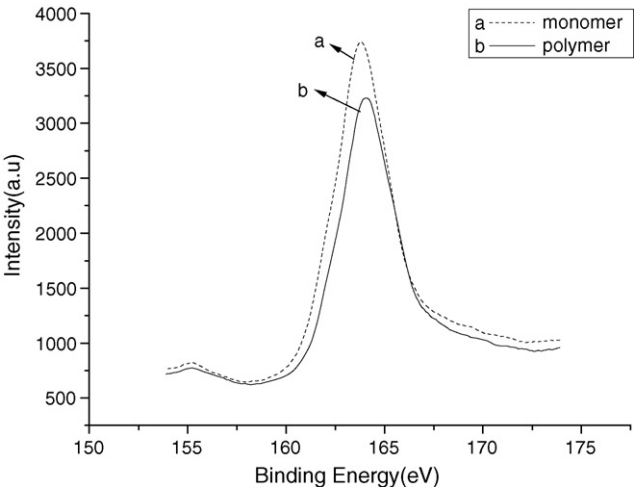

Fig. 3. XPS spectra of S_{2p} of: (a) ABTP and (b) PABTP.

3.3. XPS spectra

The XPS spectra of ABTP and PABTP gave S_{2p} peaks at band energy 164 eV, C_{1s} at 285 eV, respectively. Fig. 3 shows the XPS spectra of S_{2p}, for which the S_{2p} appear as wide peak with maximum at 163.8 and 164 eV and very weak should at 162 eV, respectively.

It was widely accepted that trithiapetalenes are substances of unusual composition having aromatic properties and resonance structure involving "single bond–no bond resonance", which depicts a resonance of cyclic structure with single bond between S–S atoms or isolated S atoms without bond at all (Scheme 2a–d) [16,17]. A family of the compounds containing trithiapetalene, trithiapenthalene antrone and the combination of fragments of trithiapetalene and antrone, were concluded having bicycle and resonance structure from XPS and quantum chemical calculations. All these compounds had similar S_{2p} wide peaks with maximum at 164 eV and should at 162 eV. On the other hand, tetrathiotetracene has the S atoms with valence of two and the S_{2p} band energy of 164 eV [18]. Hence, it can be deduced that the

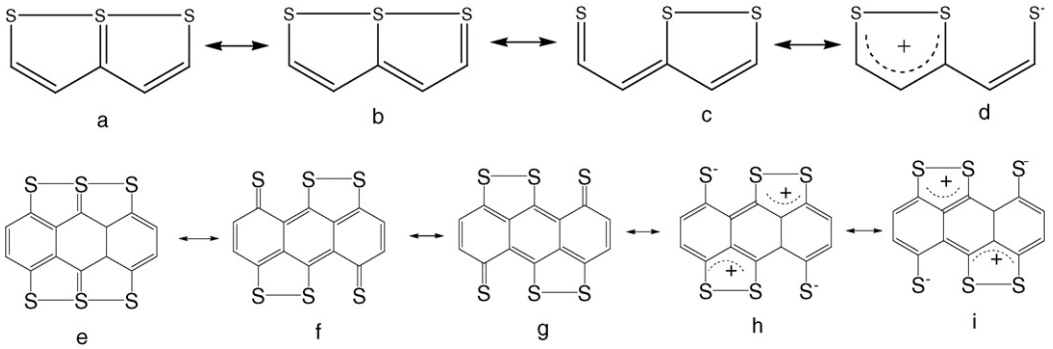

Scheme 2. The "single bond–no bond" resonance structure of trithiapetalenes ABTP.

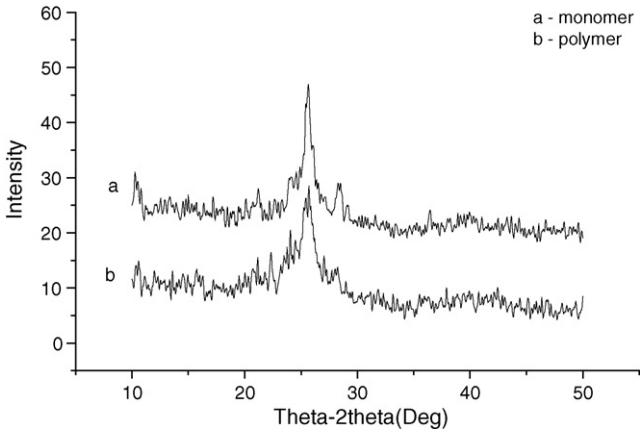

Fig. 4. X-ray diffraction spectrum of: (a) ABTP and (b) PABTP.

energy bands at 164 and 162 eV are attributed to the S atom with valence of two and four, respectively, and ABTP and PABTP have so-called "single bond–no bond" resonance (Scheme 2e–i). Therefore, ABTP may be represented by structure of (e) or (f–I) in Scheme 2.

3.4. X-ray diffraction spectra

The X-ray diffraction curves of monomer and polymer are reported in Fig. 4. Both the monomer and the polymer show strong crystalline refractions at 26° (2θ), indicating the crystalline structure. Obviously, the diffraction patterns are different from those of sulfur or anthracene and came from the new morphology of ABTP.

3.5. Charge–discharge curves

Fig. 5 shows the charge–discharge curves of PABTP, here, the discharge plateau is at ca. 2.5, 2.4 and 2.3 V on the 4th, 17th and 42nd cycle, respectively, declined gradually with the cycle number, while the charge curves showed increased voltage up to 4.4 V without plateau at all. The results mean there is some irreversible redox reaction took place during the charge–discharge process and the discharge voltage of the polymer is higher than those of elemental sulfur (2.1 V) [18].

Being used as cathode active material, the charge–discharge experiment of elemental sulfur was conducted in the same experimental condition as that of PABTP, which displayed very flat discharge voltage plateau at 2.1 V and charge voltage at 2.2–2.3 V. Obviously, the polymer has higher charge–discharge voltage than that of sulfur and very different charge–discharge behavior from sulfur.

3.6. Cycle life test

The lithium secondary batteries were built using the polymer ABTP as cathode active material and lithium as anode. The charge–discharge experiment was conducted for 77 cycles and the results shown in Fig. 6. It can be seen that the specific capacity was ca. 600 mAh g^{-1} at the 2nd–13th cycle, after a terrace of ca. 1500 mAh g^{-1} from the 20th to the 27th cycle; the capacity was maintained to ca. 800 mAh g^{-1} till the 77th cycle. The low capacity stage is a pre-activation process and the high specific capacity was obtained after activation by charging process; then the specific capacity declined slowly due to occurrence of some irreversible reaction until the new stable structure formed. In addition, the charge–discharge efficiency was above 85% for the all cycles. Generally, organodisulfides are considered too low in volume specific capacity to be used in practiced lithium batteries. But if a polymer has stable charge specific capacity of 800 mAh g^{-1} and density of 1.8 g cm^{-3}, its specific capacity in volume may reach theoretically 1400 mAh mL^{-1}, higher than that of lithium cobalt oxide ($LiCoO_2$, 750 mAh mL^{-1}).

It is surprising that the polymer PABTP has the discharge specific capacity of 800–1500 mAh g^{-1}. The generally accepted mechanism for the redox reaction of organic sulfides is the two-electron process:

$$R - S - S - R\prime \underset{-2e}{\overset{+2e}{\rightleftharpoons}} R - S^{-} + {}^{-}S - R\prime$$

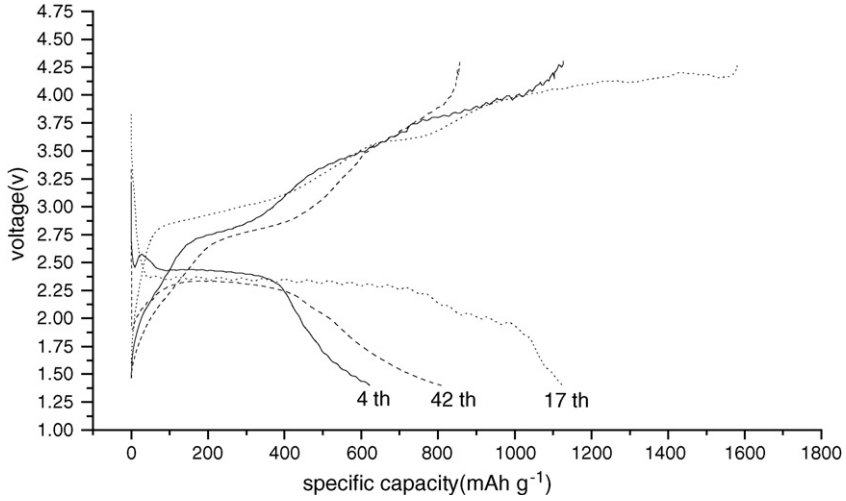

Fig. 5. The charge–discharge curves of PABTP in 1 M LiTFSI/DXL–DME (1:2) (current density 40 mA g^{-1}, cut off voltage 1.4–4.4 V).

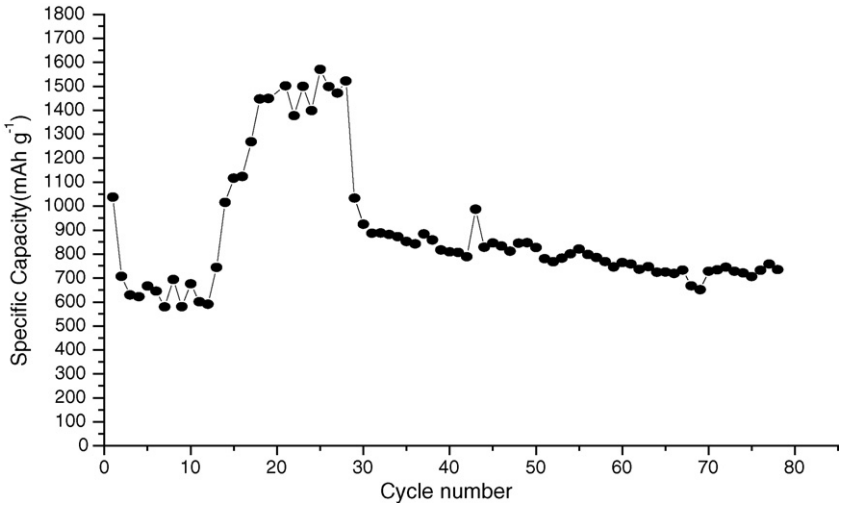

Fig. 6. Cycle life of PABTP in 1M LiTFSI/DXL–DME (1:2).

Hence, polymer PABTP would have theoretical capacity of 444 mAh g^{-1}. The capacity of 800–1500 mAh g^{-1} indicates there may be ultra redox reaction to restore electrons or novel mechanism besides the two-electron process of S–S bond.

The redox reaction of elemental sulfur can offer theoretical capacity of 1675 mAh g^{-1}:

$$S_8 \underset{-16e}{\overset{+16e}{\rightleftharpoons}} 8S^{2-}$$

A polymer–sulfur composite containing S 53.4% offered specific capacity up to 850 mAh g^{-1}, agreed with the mechanism and specific capacity of elemental sulfur [18]. In contrast, polymer PABTP containing S 58% gave specific capacity up to 1600 mAh g^{-1} and voltage ca. 2.5 V. It can be deduced that the specific capacity of the polymer is not came from and higher than those of elemental sulfur.

The mechanism is still unclear, it can be deduced that the process is complicated, involving the cooperation of the polymer, solvents, even electrolyte; the details are under investigation.

4. Conclusion

The organic sulfide polymer PABTP was synthesized and investigated as cathode active material for secondary lithium battery. The direct sulfurization of anthracene and the oxidation coupling polymerization of ABTP are facile method. The characterization by vibration spectra and XPS spectra indicated that the polymer might have "single bond–no bond" resonance structure similar to trithiapentalene. The charge–discharge tests of the polymer performed at ambient condition show that the polymer had unusually high discharge specific capacity up to 1500 mAh g^{-1}. The high charge–discharge voltage illustrated that the redox reaction resulted from the polymer other than free sulfur. In addition, the polymer is easy to prepare, low cost and environmentally benign. The mechanism of the redox reaction is still under investigation.

Acknowledgement

Project 20274031 supported by NNSFC.

References

[1] S.J. Visco, C.C. Maihe, L.C. De Jonghe, M.B. Armand, J. Electrochem. Soc. 136 (1989) 661–664.
[2] M. Liu, S.J. Visco, L.C. De Jonghe, J. Electrochem. Soc. 138 (1991) 1891–1895.
[3] M. Liu, S.J. Visco, L.C. De Jonghe, J. Electrochem. Soc. 138 (1991) 1896–1901.
[4] M.M. Doeff, M.M. Lerner, S.J. Visco, L.C. De Jonghe, J. Electrochem. Soc. 139 (1992) 2077–2081.
[5] M.M. Doeff, S.J. Visco, L.C. De Jonghe, J. Appl. Electrochem. 22 (1992) 307–309.
[6] P. Novak, K. Muller, K.S.V. Santhanam, O. Haas, Chem. Rev. 97 (1997) 207–281.
[7] S. Panero, P. Prosperi, F. Bonino, B. Scrosati, Electrochim. Acta 32 (1987) 1007–1011.
[8] J. Desilvestro, W. Scheifele, O. Haas, J. Electrochem. Soc. 139 (1992) 2727–2736.
[9] K. Naoi, S. Suematsu, M. Komiyama, N. Ogihara, Electrochim. Acta. 47 (2002) 1091–1096.
[10] L.J. Xue, J.X. Li, S.Q. Hu, M.X. Zhang, Y.H. Zhou, C.M. Zhan, Electrochem. Commun. 5 (2003) 903–906.
[11] P. Frére, J. Raimundo, P. Blanchard, J. Delaunay, P. Richomme, J. Sauvajol, J. Orduna, J. Garin, J. Roncali, J. Org. Chem. 68 (2003) 7254–7265.
[12] G. Zerbi, M. Veronelli, S. Martina, A.-D. Schlûtter, G. Wegner, Adv. Mater. 6 (1994) 385–388.
[13] V. Hernandez, C. Castiglioni, M. Del Zoppo, G. Zerbi, Phys. Rev. B 50 (1994) 9815–9823.
[14] H.E. Schaffer, R.R. Chance, R.J. Silbey, K. Knoll, R.R. Schrock, J. Chem. Phys. 94 (1991) 4161–4170.
[15] Q. Shen, K. Hedberg, J. Am. Chem. Soc. 96 (1974) 289–291.
[16] R. Cimiraglia, H.J. Hofimann, J. Am. Chem. Soc. 113 (1991) 6449–6451.
[17] T.M. Ivanova, S.V. Zaharov, B.E. Zaitsev, M.A. Ryabov, O.V. Kovalchoukova, J. Electron. Spectrosc. Relat. Phenom. 137–140 (2004) 457–462.
[18] J. Wang, J. Yang, J. Xie, N. Xu, Adv. Mater. 14 (2002) 963–965.